Higgs decays to bosons
ATLAS results

Stefano Rosati

INFN Roma

24 July 2017

On behalf of the ATLAS Collaboration

Introduction

- Bosonic channels analyses in ATLAS
  - $H \to ZZ^* \to l^+l^-l^+l^-$
  - $H \to \gamma\gamma$
- Mass measurement
- Fiducial and differential cross sections
- Couplings
- Results shown here are based on 36.1 fb^{-1} of $\sqrt{s} = 13\ \mathrm{TeV}$ p-p collision data collected by the ATLAS experiment in 2015 and 2016
- Focusing on the channels with new most recent updates
- All results from the recent ATLAS CONF-notes:
  - ATLAS-CONF-2017-046
  - ATLAS-CONF-2017-045
  - ATLAS-CONF-2017-043
  - ATLAS-CONF-2017-032

Higgs to four leptons event selection

- Four opposite sign, same flavour leptons (μ,e), with $p_T > 20, 15, 10, 5(\mu)/7(e)$ GeV, isolated and from the primary vertex
- Cut on the two di-lepton mass pairs
- BDT discriminant to reduce ZZ background, based on p_T^{4l}, η^{4l} and $D_{ZZ} = ln(|M_{HZZ^*}|^2/|M_{ZZ^*}|^2)$
- Z-mass constraint on the leading lepton pair
- Jets: anti-k_t algorithm with R=0.4, $p_{\mathrm{T}} > 30$ GeV

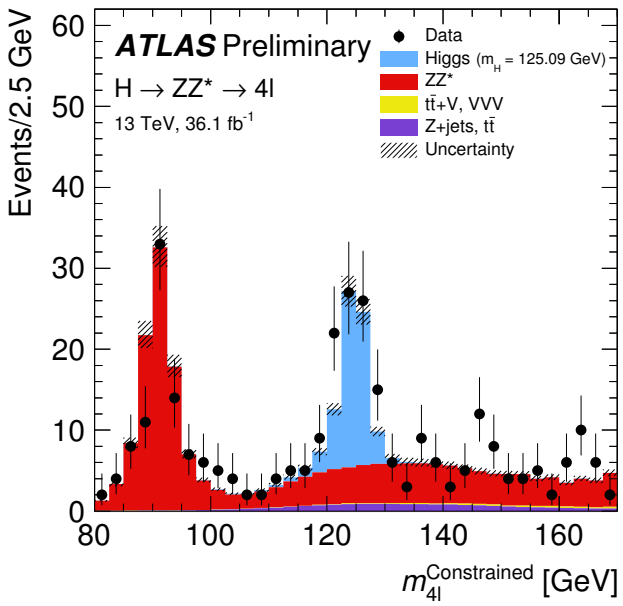

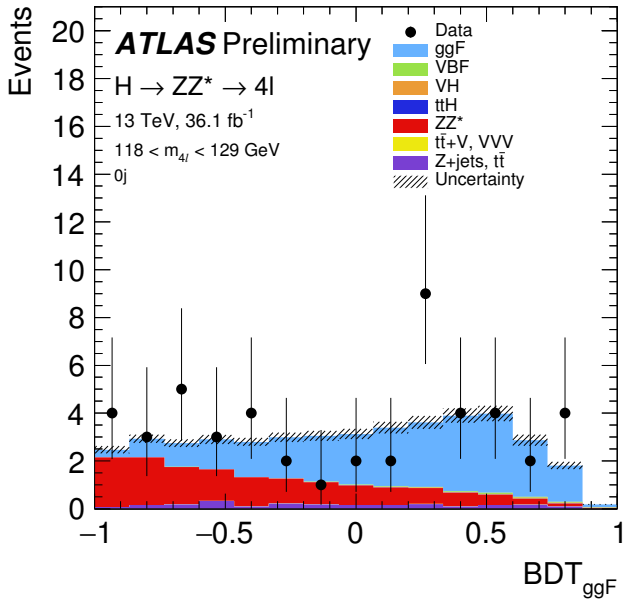

Higgs to two photons event selection

- Two photons with $E_T/m_{\gamma\gamma} > 0.35, 0.25$ in $|\eta| < 2.37$, ($1.37 \leq |\eta| \leq 1.52$ excluded)
- Neural network combining photons directions and information from the Inner Detector for primary vertex identification
  - Rate of correct diphoton vertex selection in MC is 79% for gg-fusion events, 84-97% for other production mechanisms
- Keep events with $105\ \mathrm{GeV} \leq m_{\gamma\gamma} \leq 160\ \mathrm{GeV}$
- Jets: anti-k_t algorithm with R=0.4, $p_{\mathrm{T}} > 30\ \mathrm{GeV}$
- Selected events are categorized:
  - Use 31 categories sensitive to the production mode
  - Same categorization scheme for the mass measurement

MASS MEASUREMENT

Muon and e/γ calibrations

- Muon momentum scale and resolution calibration on $J/\psi \to \mu^+\mu^-$ and $Z \to \mu^+\mu^-$
  - Scale systematics between $\sim$ 0.05% and $\sim$ 0.2%
  - Correction for sagitta measurement bias due to ID misalignments (affects resolution)
- Electron scale measured on $Z \to e^+e^-$ and cross-checked on $J\psi \to e^+e^-$. Photon scale cross-checked on $Z \to l^+l^-\gamma$
  - γ scale uncertainty at $\sim$60 GeV is 0.4% (barrel) and 0.8% (endcap)
  - e uncertainty at 40 (10) GeV is 0.02% (0.5%) in the barrel and 0.1% (0.8%) in the endcap

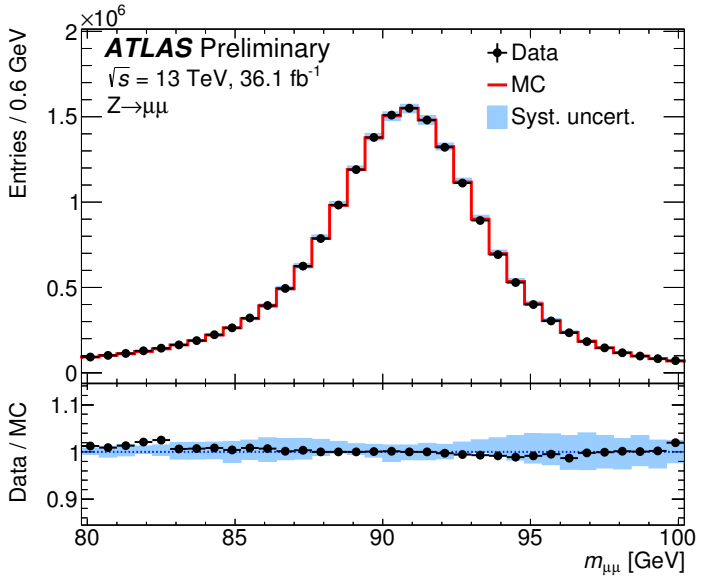

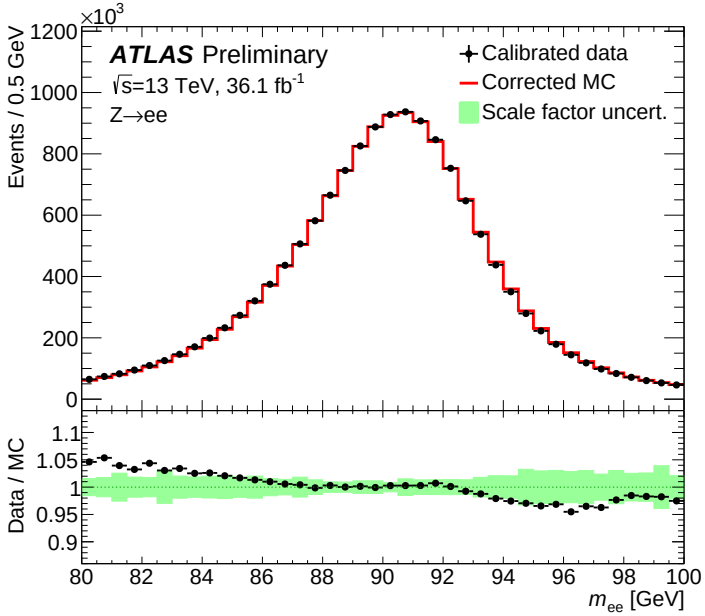

Mass fit in the 4l channel

- Four exclusive categories in BDT bins (∼6% resolution improvement)
- Z mass constraint applied to the leading lepton pair (∼15% resolution improvement)
- Mass model as convolution of a BW with SM width, with a resolution function calculated per-event based on single-lepton resolutions
- Validation on $Z \to 4l$ events

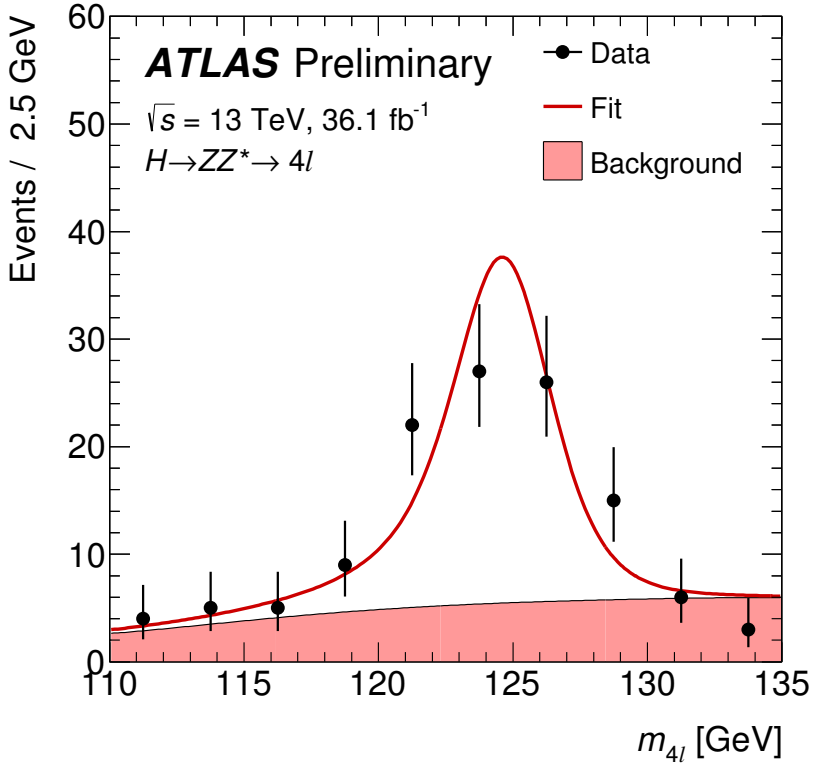

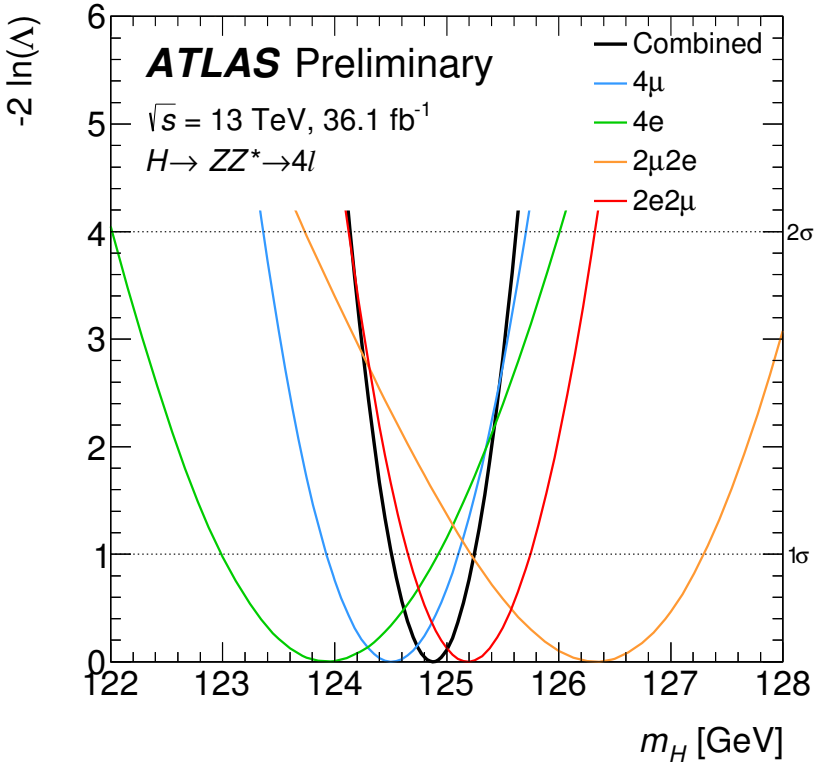

Mass fit in the $\gamma\gamma$ channel

- Signal model is a double-sided Crystal Ball function
  - Parameters dependence on m_H from samples weighted for production modes
  - Resolution ranging from 1.42 GeV to 2.14 GeV (1.87 GeV inclusive)
- Background parametrized with a continuous function for each category
  - Function chosen as the one that minimizes the fitted signal yield in a background-only sample (from CR or from MC)
  - Typically exponential for low-stat categories, power-law or exp of polynomial for the others

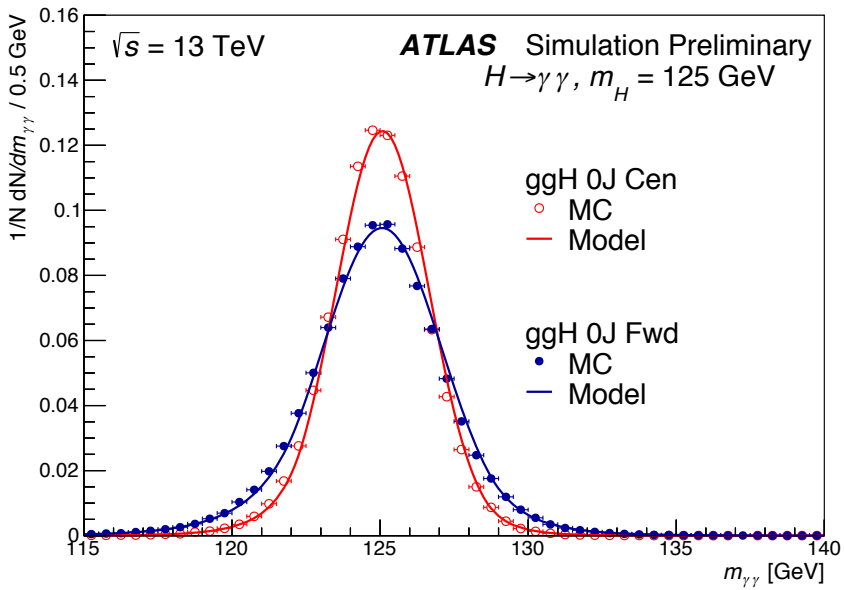

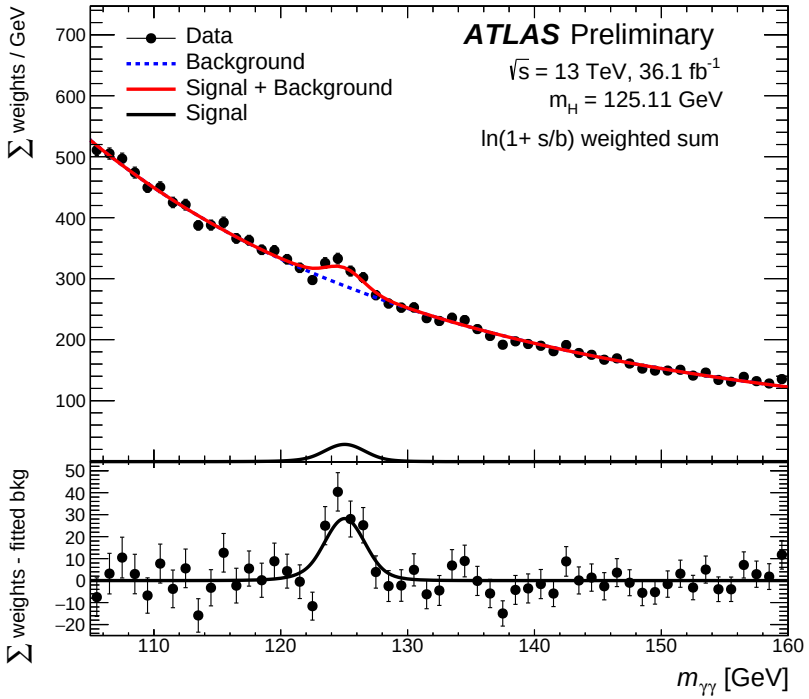

Mass fit results

- 4l mass fit:
  $m_H^{ZZ^*} = 124.88 \pm 0.37(\text{stat}) \pm 0.05(\text{syst})\ \text{GeV} = 124.88 \pm 0.37\ \text{GeV}$
- $\gamma\gamma$ mass fit:
  $m_H^{\gamma\gamma} = 125.11 \pm 0.21(\text{stat}) \pm 0.36(\text{syst})\ \text{GeV} = 125.11 \pm 0.42\ \text{GeV}$
- The combined measurement will be presented by Bruno Mansoulié tomorrow

Systematics for m_{4l}

Source	Unc. [MeV]
Muon momentum scale	40
Electron energy scale	20
Background modelling	10
Simulation statistics	8

Systematics for $m_{\gamma\gamma}$

Source	Unc. [MeV]
LAr cell non-linearity	± 200
LAr layer calibration	± 190
Non-ID material	± 120
Lateral shower shape	± 110
ID material	± 110
Conversion reconstruction	± 50
$Z \to ee$ calibration	± 50
Background model	± 50
Primary vtx	± 40
Resolution	$^{+20}_{-30}$
Signal model	± 20

CROSS SECTIONS AND COUPLINGS

Simplified template cross-sections

- Production cross section times BR is measured in mutually exclusive phase space regions (production bins), with $|y_H| < 2.5$
- Chosen to maximise the measurement precision and the sensitivity to BSM contributions

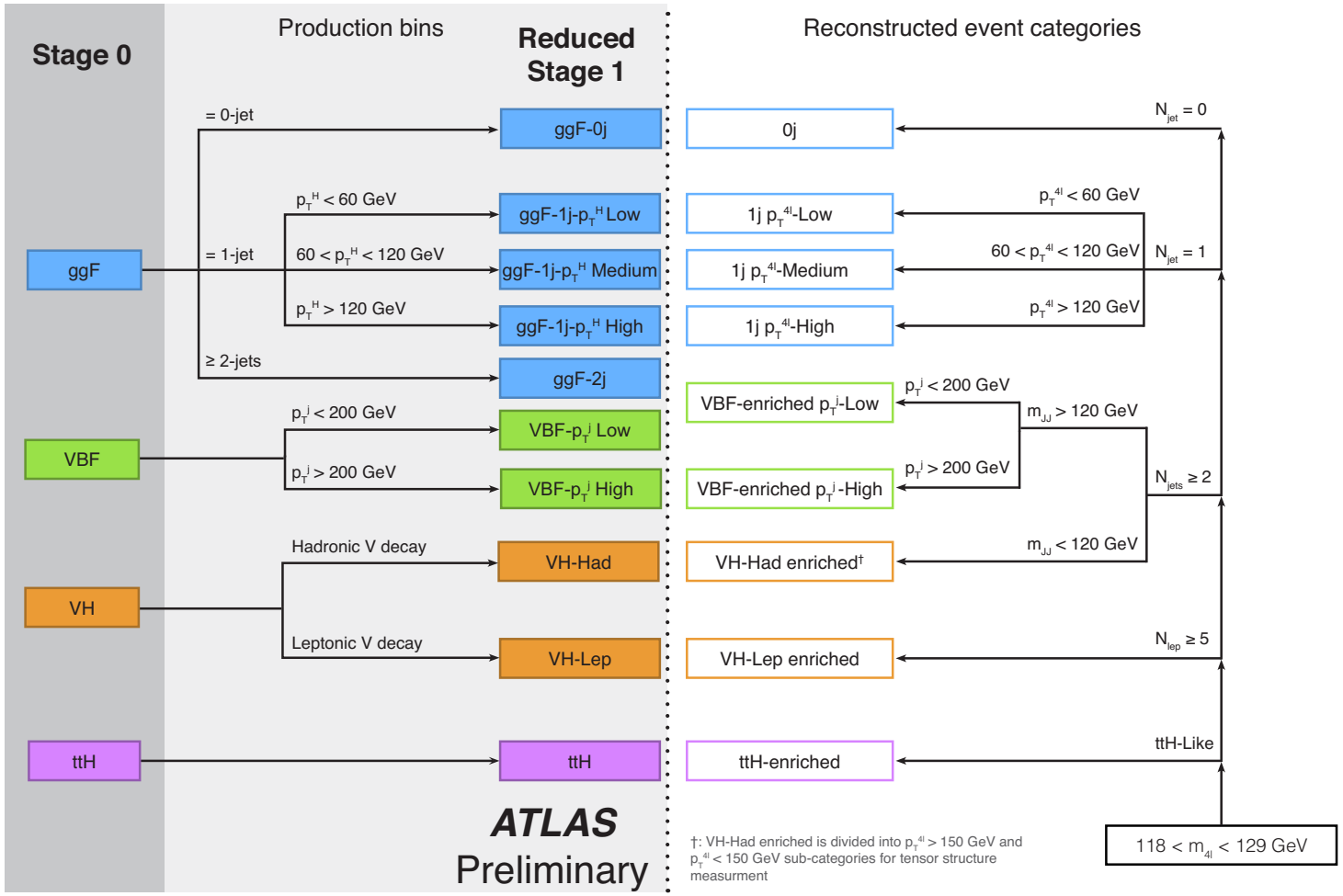

Categorization of reconstructed candidates

$H \to ZZ^* \to l^+l^-l^+l^-$ categorization

- Based on the presence of b-jets, jets and additional leptons in the event
- Further categorization based on kinematic cuts on p_{T}^{4l}, p_{T}^{j1}, m_{jj}
- End up with 9 categories each enriched in one or more production process
- Further separation using multi-variate discriminants in the categories with enough statistics, to select ggF, VBF, VH-hadronic

$H \to \gamma\gamma$ categorization

- 31 exclusive categories each enriched in one of the production mechanisms
- Dedicated BDT used for VBF- and ttH-enriched categories to increase the separation from ggF and background

Cross sections by production mode: 4l channel

- Global signal strength:
  $\mu = 1.28^{+0.18}_{-0.17}(\text{stat.})^{+0.08}_{-0.06}(\text{exp.})^{+0.08}_{-0.06}(\text{th.}) = 1.28^{+0.21}_{-0.19}$

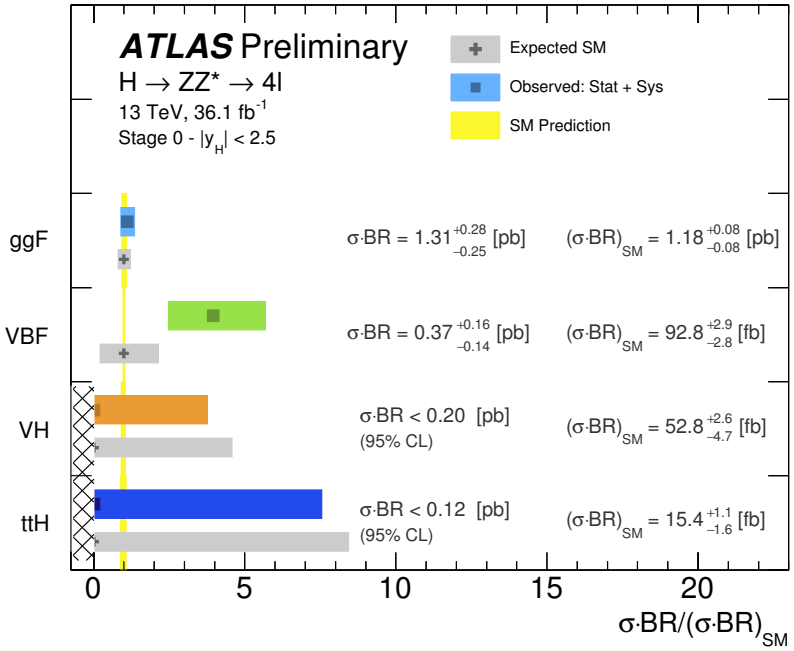

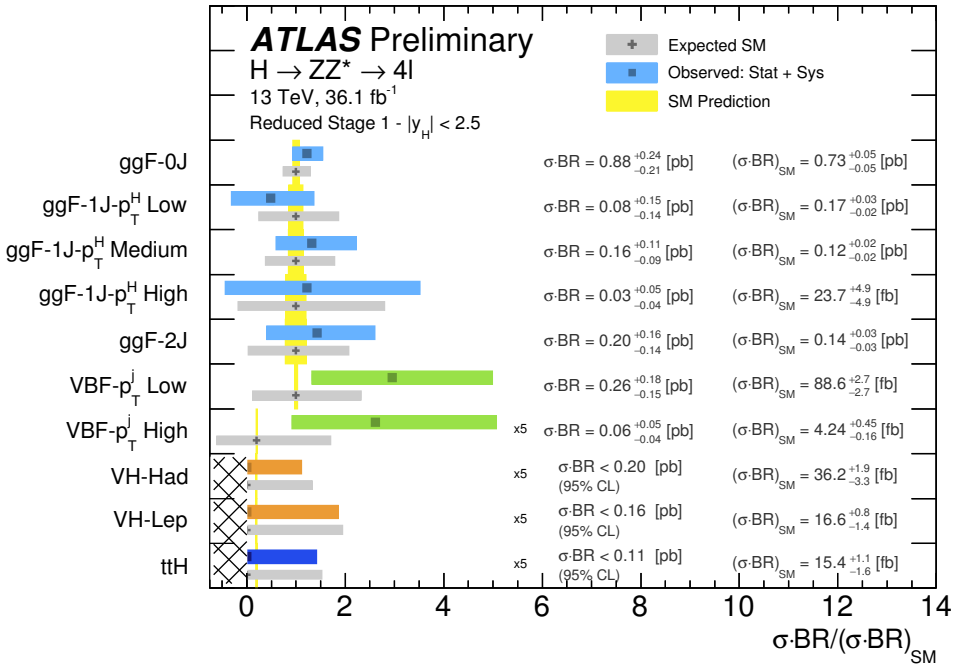

Cross sections by production mode: $\gamma\gamma$ channel

- Global signal strength:
  $\mu = 0.99^{+0.12}_{-0.11}(\text{stat})^{+0.06}_{-0.05}(\text{exp.})^{+0.06}_{-0.05}(\text{th.}) = 0.99 \pm 0.14$

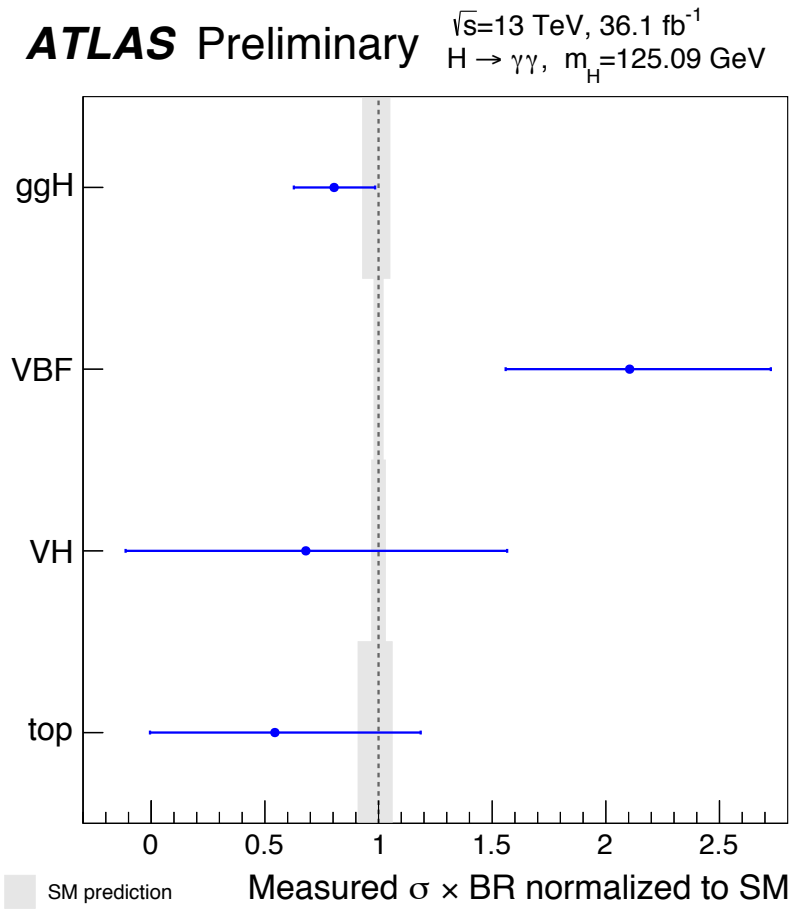

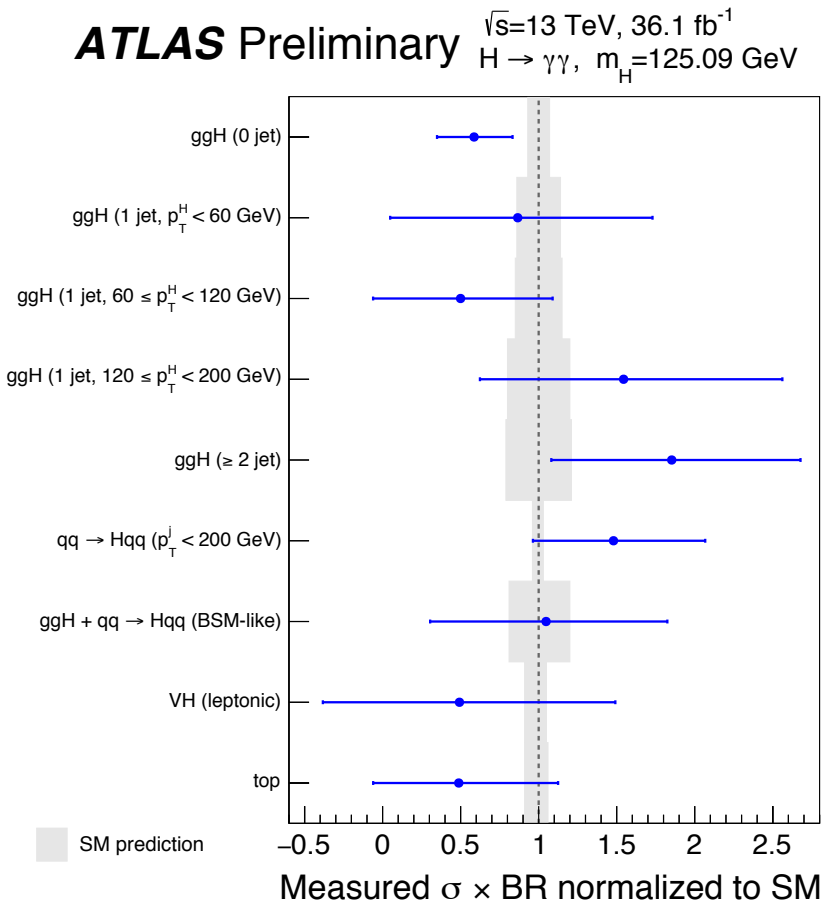

Tensor structure of couplings

- The tensor structure of couplings is studied in 4l within the framework of the effective Lagrangian of the Higgs characterization model **[JHEP 1311 (2013) 043]**
- Couplings fit based on the event yields in each of the 4l experimental categories
- Fits with $k_{SM} = 1$ (SM coupling factor) fixed. Difference with respect to the SM expectation is mostly caused by the excess in the 2-jet category. Max deviation is 2.3σ for k_{HVV}.

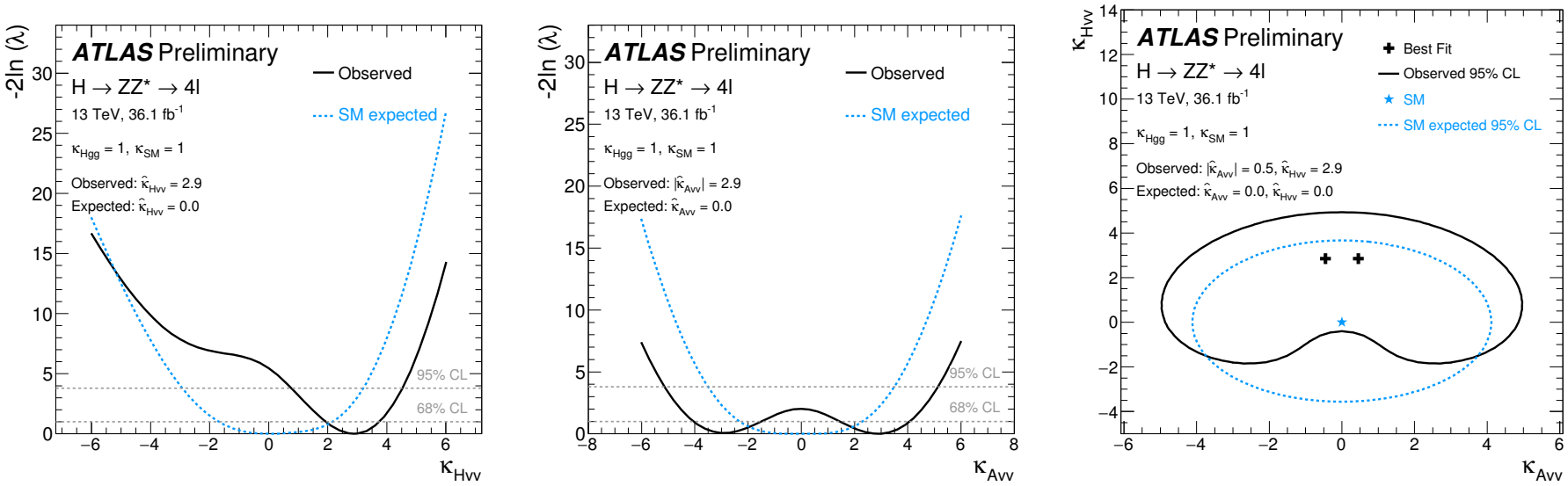

- Agreement with the SM hypothesis improves if k_{SM} is left free in the fit

Fiducial and total cross sections

- Fiducial volume: cuts based on detector acceptance, to minimize model dependency in the extrapolation
- Corrections applied for detector effects: bin by bin unfolding as correction factors

$$\sigma_{i,fid} = \sigma_i \times A_i \times BR = \frac{N_{i,fit}}{L \times C_i}$$

  - $\sigma_i \rightarrow$ total cross section
  - $A_i \rightarrow$ acceptance
  - $C_i \rightarrow$ correction factor

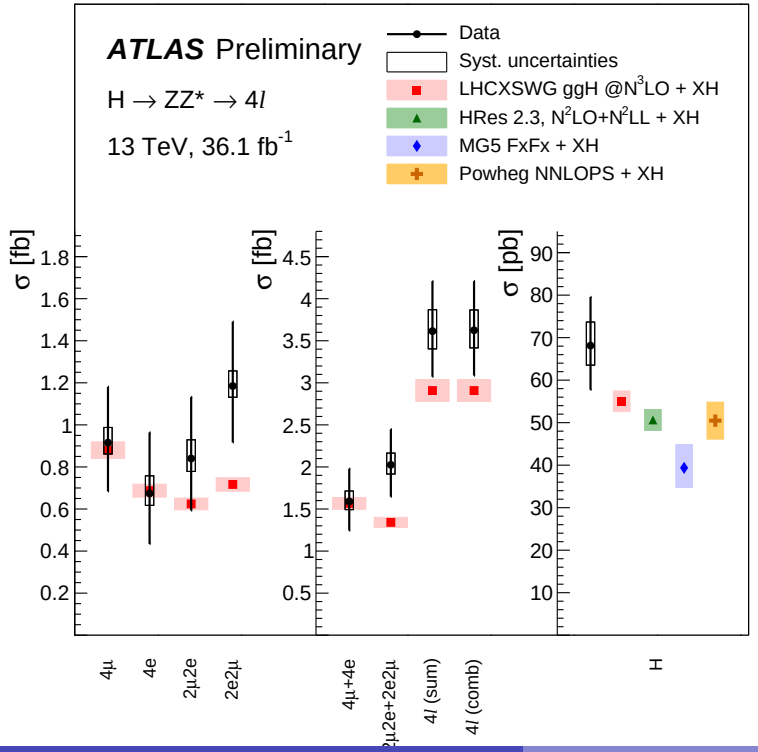

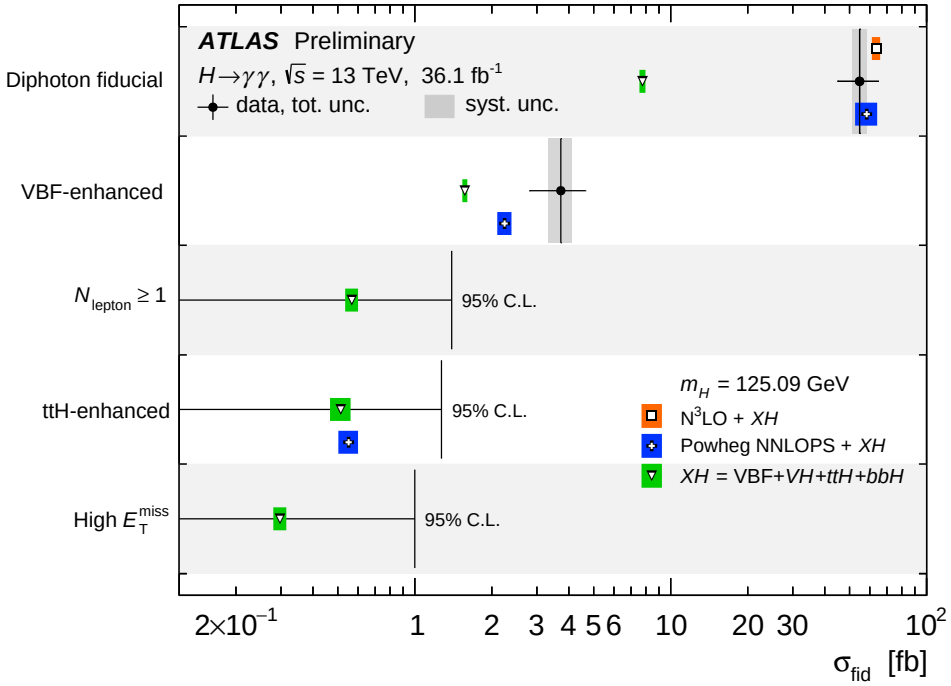

Differential cross sections: p_T

- The differential p_T distribution is sensitive to perturbative QCD calculations and presence of new additional particles in loops
- Agreement with the SM (NNLOPS): p-value 25% for 4l, 51% for $\gamma\gamma$

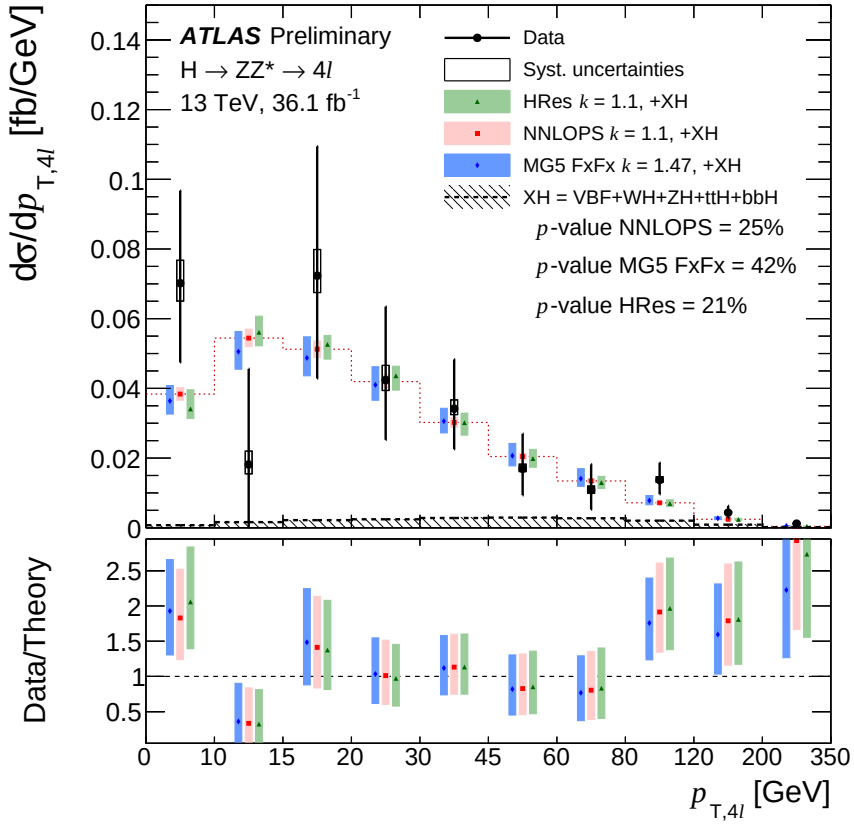

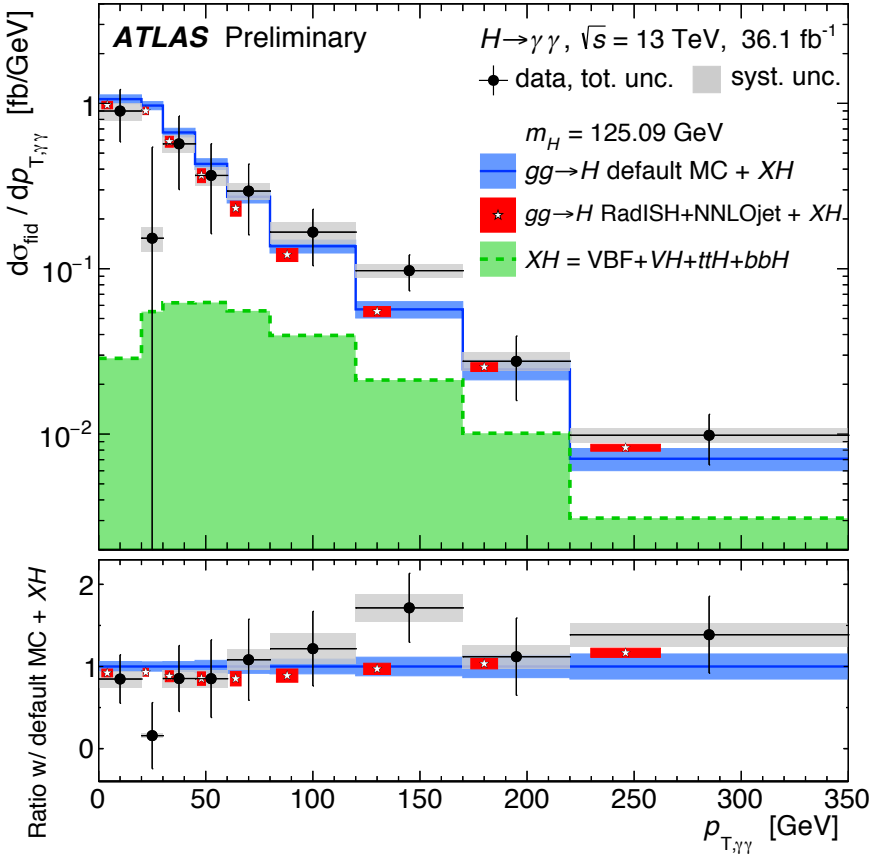

Differential cross sections: N_{jets} and $|y_{\gamma\gamma}|$

- Sensitive to production mode composition and PDFs

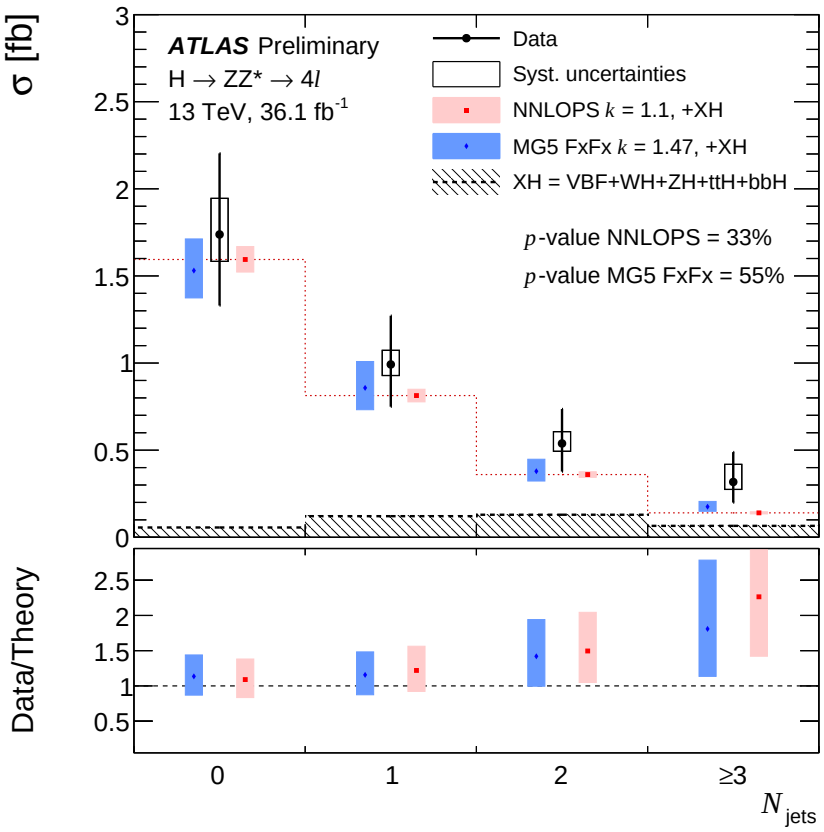

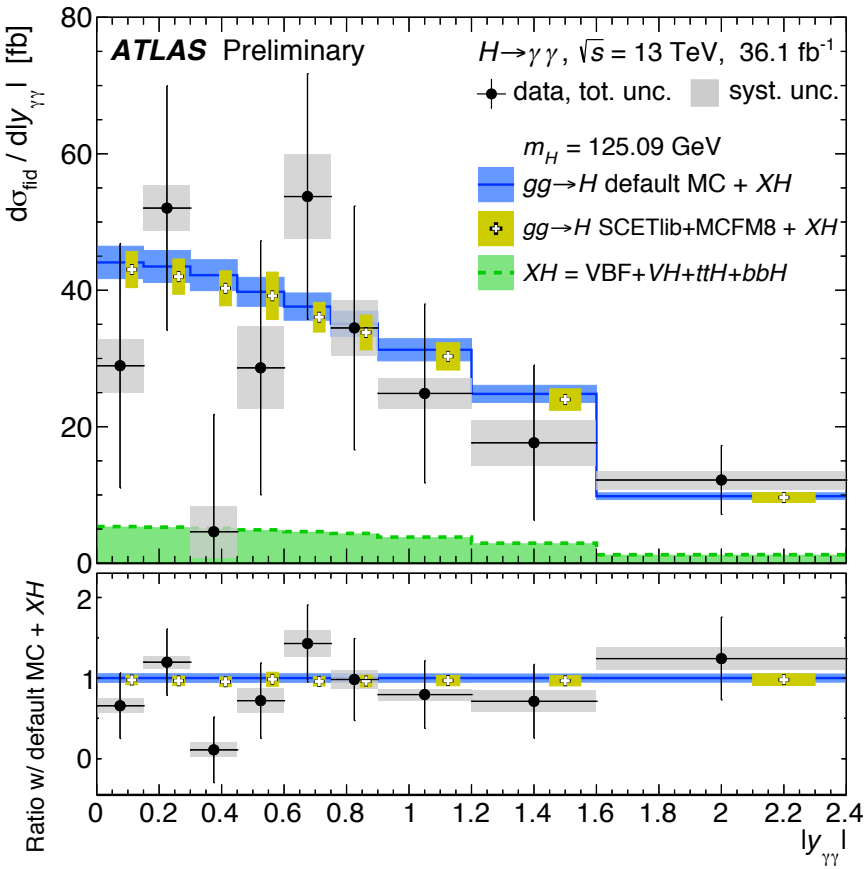

Limits on contact-interaction decay terms

- Terms modifying the contact-interaction between the Higgs and left- and right-handed leptons
  - Lepton universality assumed

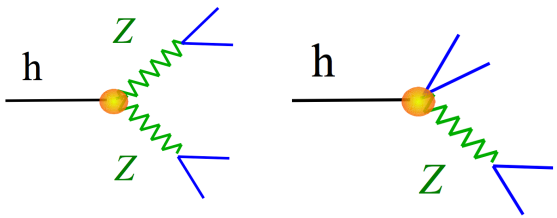

- Double-differential cross section in the m_{12}, m_{34} plane used to extract limits in the pseudo-observables framework **[Eur. Phys. J. C (2015) 75: 128]**
  - The differential information helps in constraining the couplings more than the total cross section alone

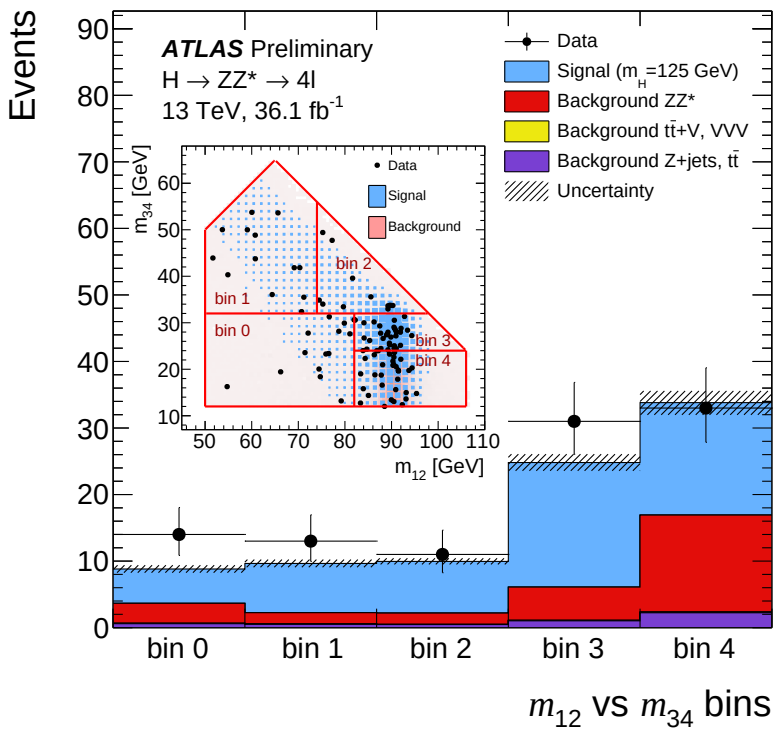

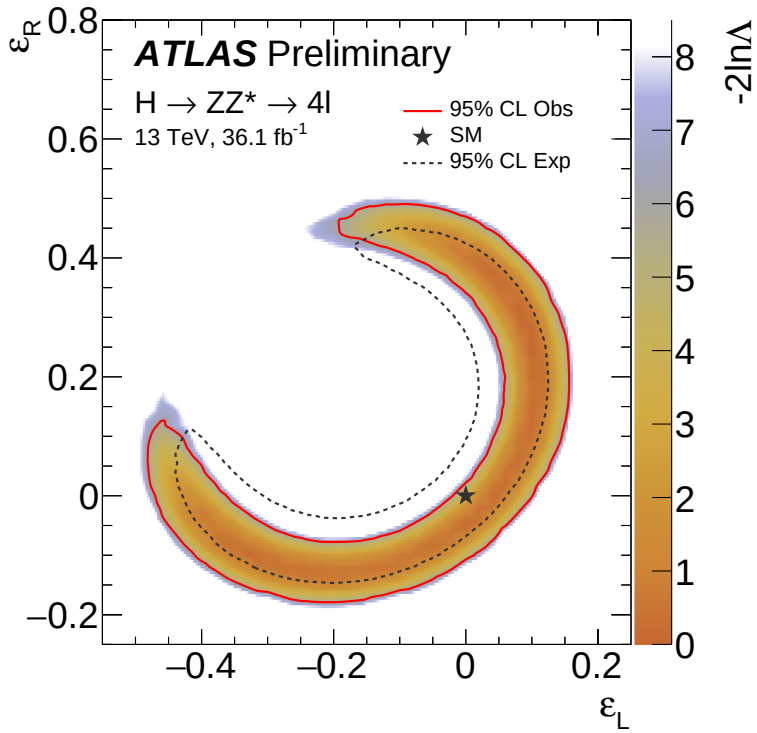

Conclusions

- The most recent results on $H \to ZZ^* \to l^+l^-l^+l^-$ and $H \to \gamma\gamma$ decay channels have been presented, based on the analysis of 36.1 fb^{-1} of data collected at $\sqrt{s} = 13$ TeV in 2015 and 2016
- Mass measurement
  - Based on the latest calibrations for muons, electrons and photons, and improved analysis techniques
  - Result in excellent agreement with the Run-1 ATLAS+CMS combination
- Updated cross section measurement per production mechanism
- Fiducial total and differential cross sections and extrapolations to the full phase-space
- First limits on contact interaction terms and updated limits on Higgs characterization effective couplings
- No deviation from the SM is observed
- Most of the measurements are limited by statistics
- See the talk tomorrow by B. Mansoulié on the combination of ATLAS measurements

BACKUP SLIDES

Electron and photon scale calibration

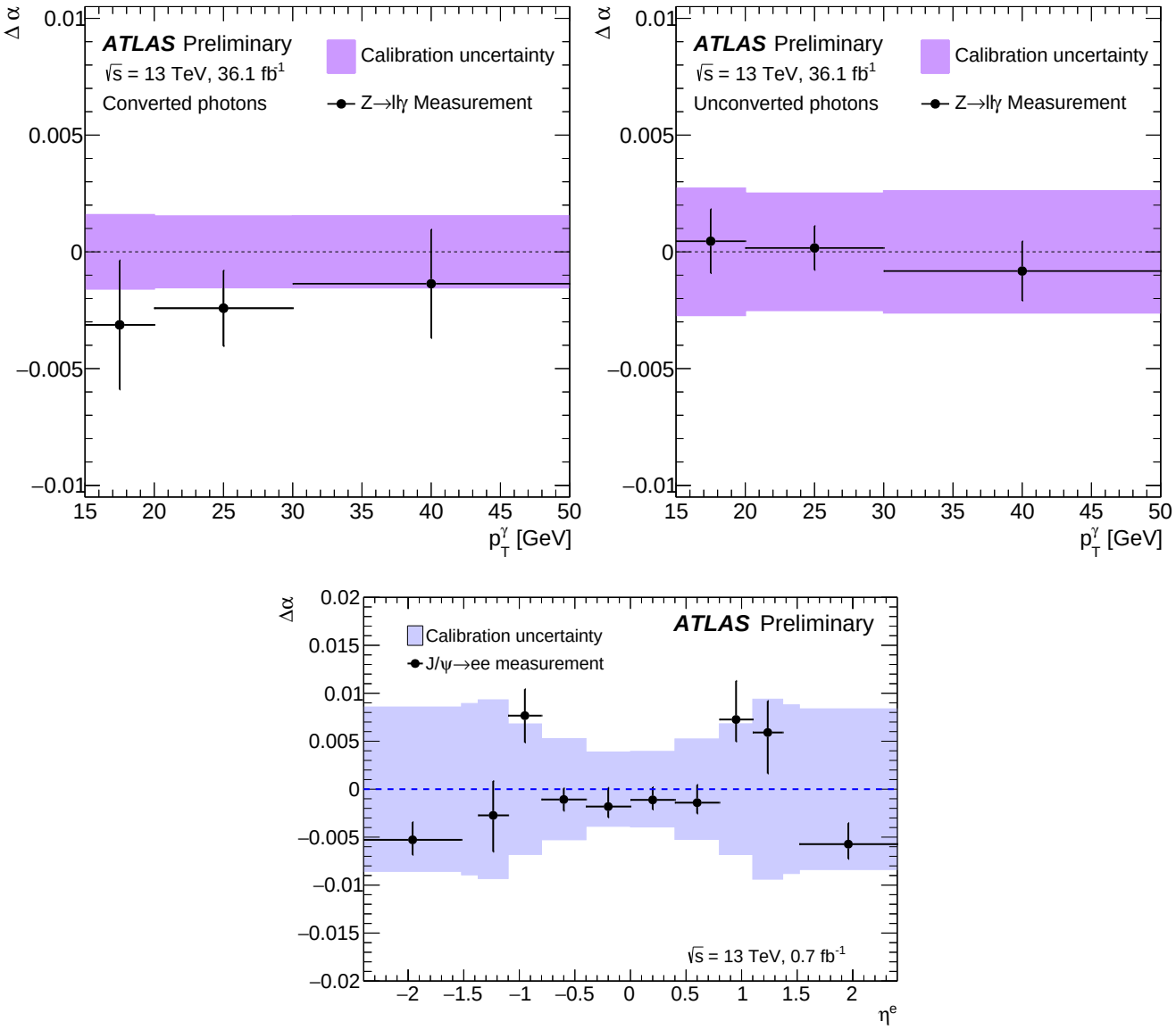

Muon scale calibration

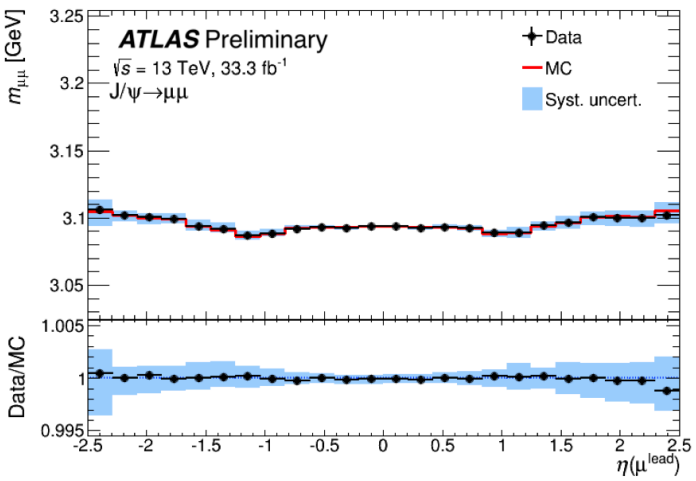

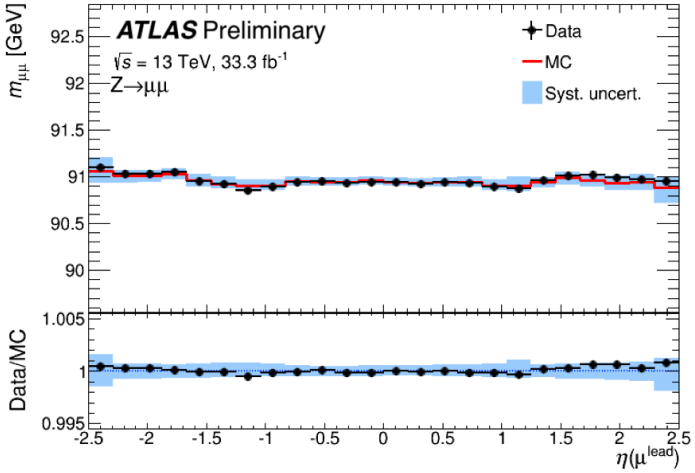

Mass fit per channel

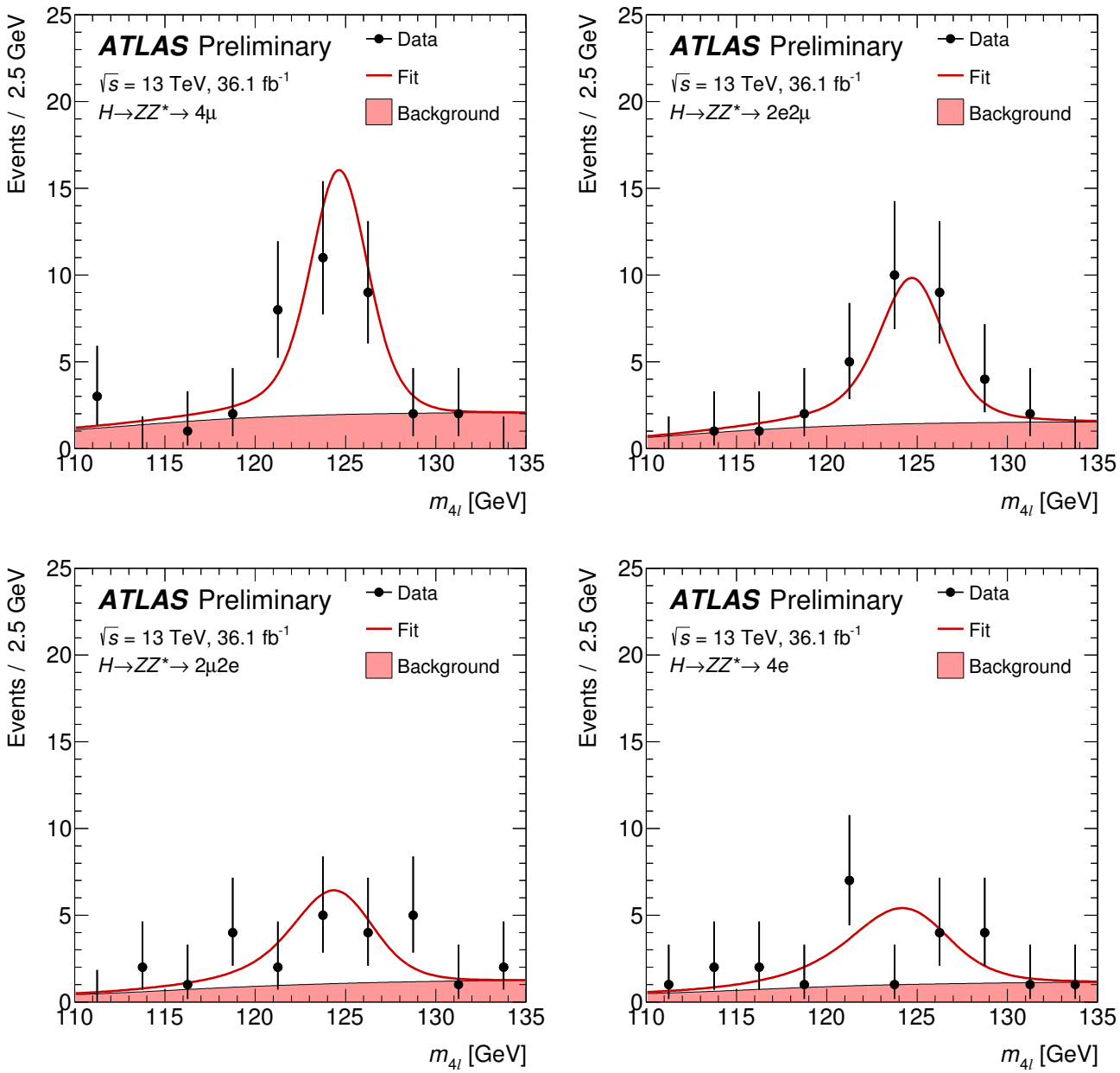

Z→4l mass fits

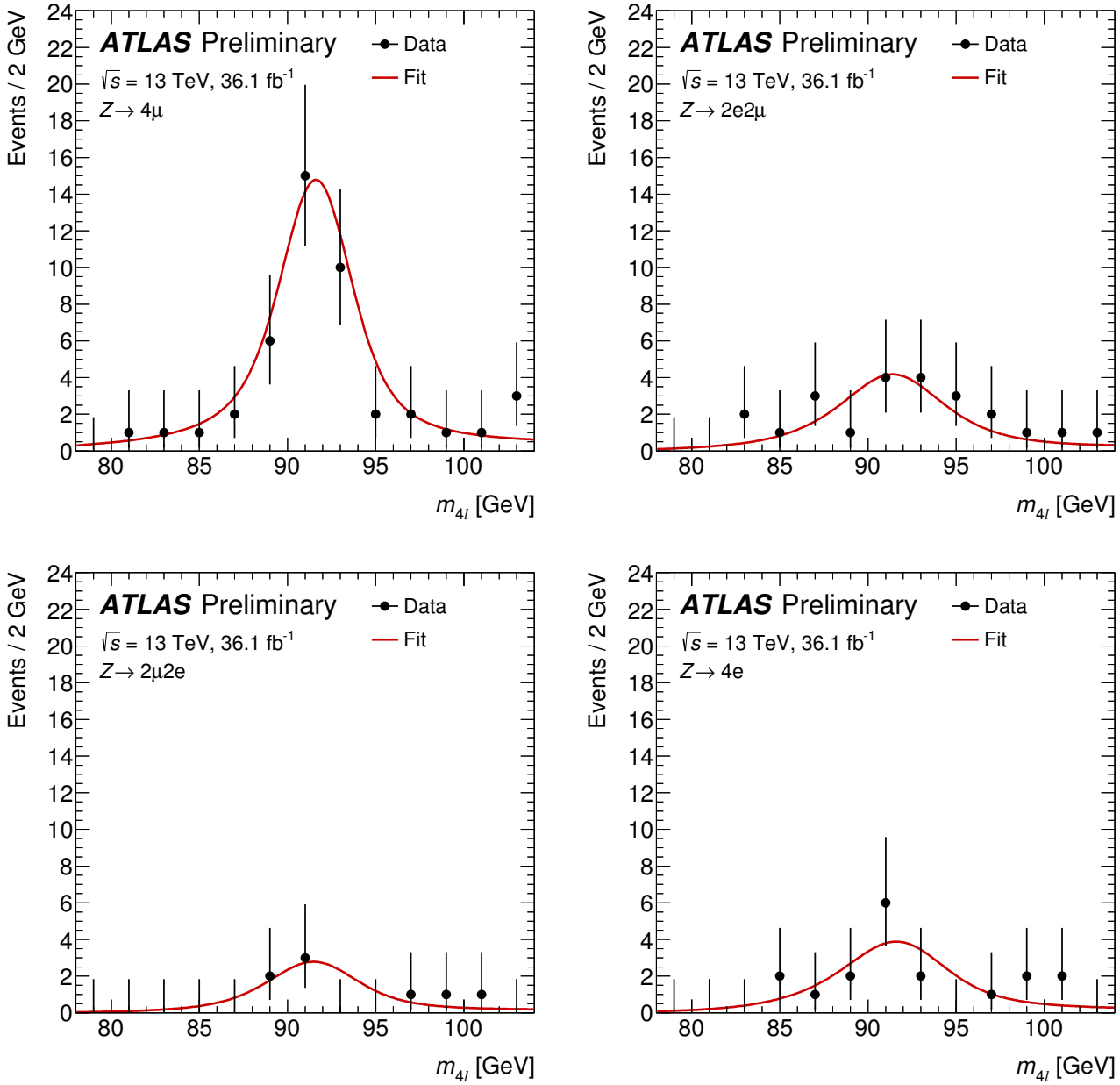

Sagitta bias correction

- Correct the effects of local ID misalignments, that are causing local charge-dependent biases on the muon sagitta measurement
- Improvement of Z mass resolution by 1% to 5%, depending on the η and ϕ of the muons in the pair

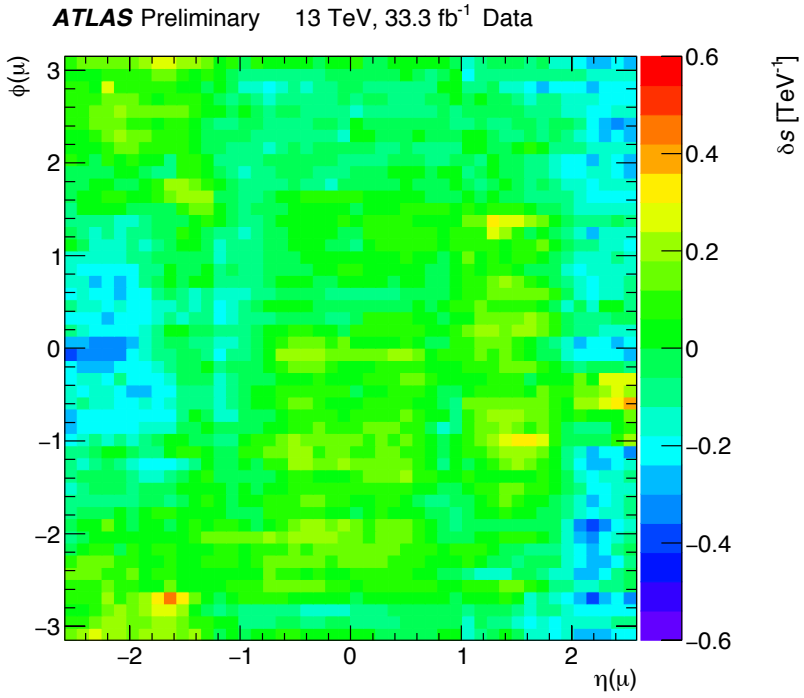

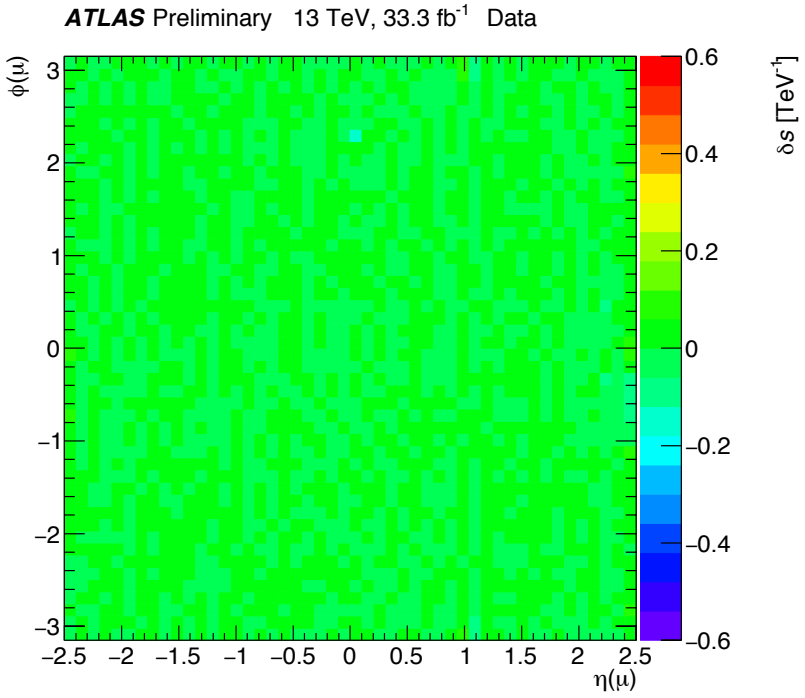

Differential cross sections

- m_{34} for the 4l channel and $cos(\theta^*)$ for $\gamma\gamma$

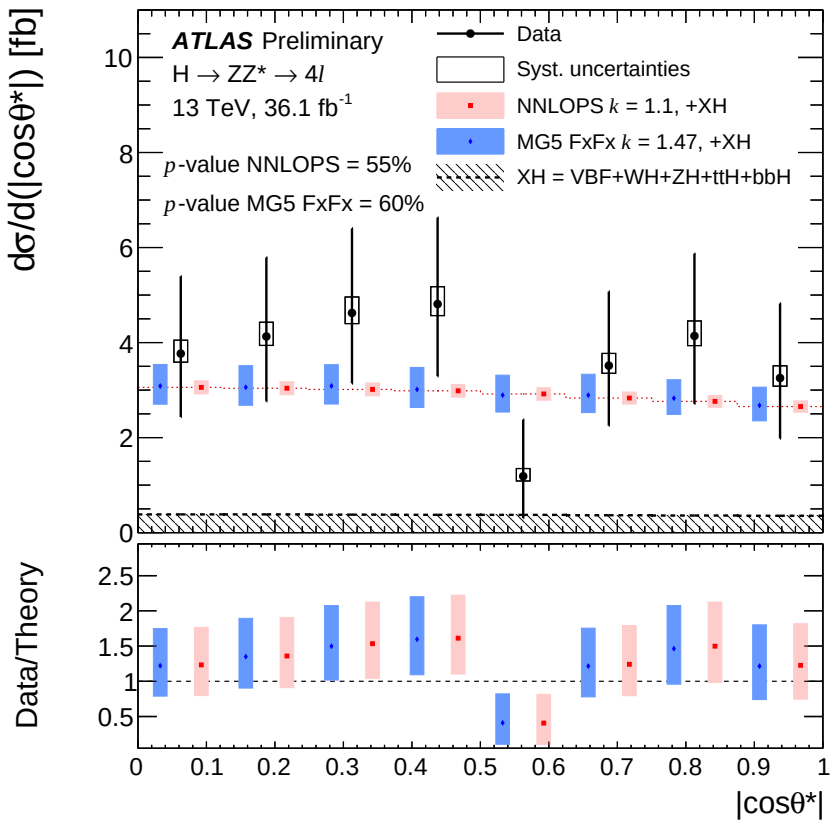

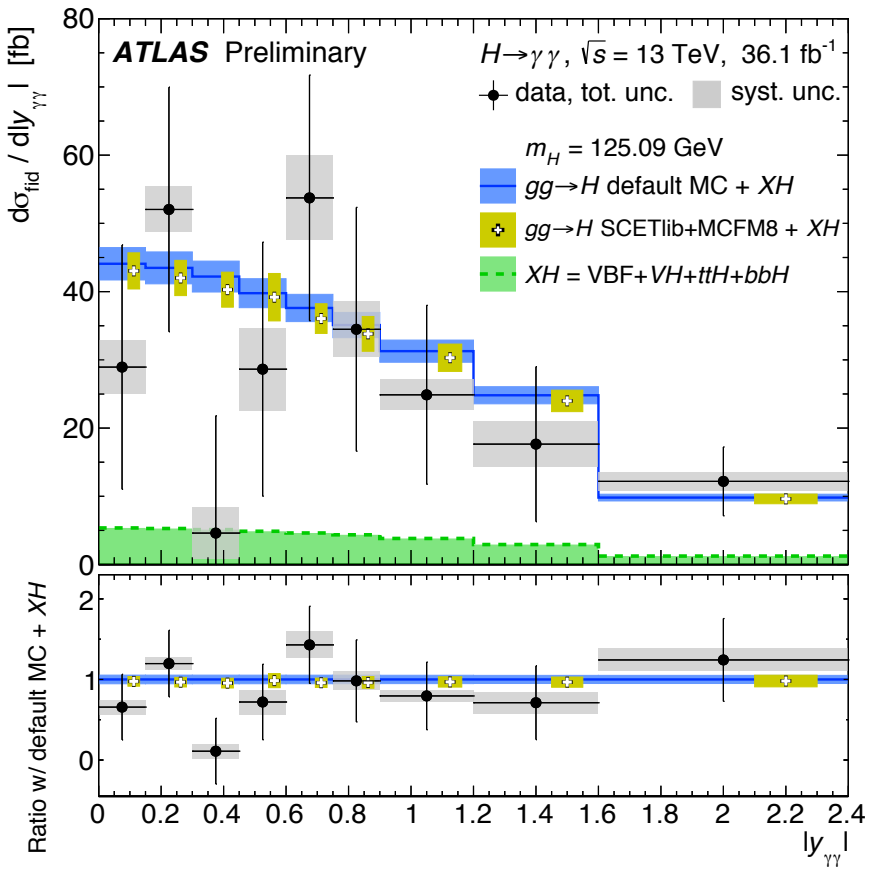

Expected and observed events in the 4l channel

Decay channel	Signal (full mass range)	Signal	ZZ^*	Other backgrounds	Total expected	Observed
4μ	21.0 ± 1.7	19.7 ± 1.6	7.5 ± 0.6	1.00 ± 0.21	28.1 ± 1.7	32
$2e2\mu$	15.0 ± 1.2	13.5 ± 1.0	5.4 ± 0.4	0.78 ± 0.17	19.7 ± 1.1	30
$2\mu 2e$	11.4 ± 1.1	10.4 ± 1.0	3.57 ± 0.35	1.09 ± 0.19	15.1 ± 1.0	18
$4e$	11.3 ± 1.1	9.9 ± 1.0	3.35 ± 0.32	1.01 ± 0.17	14.3 ± 1.0	15
Total	59 ± 5	54 ± 4	19.7 ± 1.5	3.9 ± 0.5	77 ± 4	95

Reconstructed category	N_S Expected	N_S Observed	Acceptance [%] ggF	VBF	VH	ttH	bbH
$0j$, BDT-Bin 0-4	5^{+4}_{-3}	10^{+5}_{-4}	2.40 ± 0.23	0.178 ± 0.029	0.20 ± 0.05	–	2.0 ± 1.0
$0j$, BDT-Bin 5-9	11 ± 4	11 ± 4	5.4 ± 0.5	0.64 ± 0.12	0.74 ± 0.11	–	6.3 ± 3.2
$0j$, BDT-Bin 10-14	11^{+4}_{-3}	12^{+4}_{-3}	5.2 ± 0.6	1.03 ± 0.28	1.89 ± 0.27	–	5.6 ± 2.8
$1j$ $p_T^{4\ell}$-Low, BDT-Bin 0-4	$5.8^{+3.2}_{-2.6}$	$7.6^{+3.5}_{-2.9}$	2.7 ± 0.4	1.25 ± 0.10	1.72 ± 0.19	–	3.1 ± 1.6
$1j$ $p_T^{4\ell}$-Low, BDT-Bin 5-9	$3.1^{+2.4}_{-1.8}$	$0.8^{+1.8}$	1.33 ± 0.20	2.02 ± 0.12	0.85 ± 0.09	–	1.4 ± 0.7
$1j$ $p_T^{4\ell}$-Med, BDT-Bin 0-4	$3.5^{+2.5}_{-1.8}$	$5.1^{+2.8}_{-2.1}$	1.53 ± 0.25	1.41 ± 0.23	2.09 ± 0.25	–	1.0 ± 0.5
$1j$ $p_T^{4\ell}$-Med, BDT-Bin 5-9	$2.0^{+1.9}_{-1.2}$	$2.6^{+2.1}_{-1.4}$	0.74 ± 0.11	2.68 ± 0.27	0.49 ± 0.05	–	0.27 ± 0.14
$1j$ $p_T^{4\ell}$-High	$1.5^{+1.7}_{-1.0}$	$2.8^{+2.1}_{-1.4}$	0.56 ± 0.12	1.74 ± 0.24	1.06 ± 0.10	–	0.17 ± 0.09
VBF-enriched p_T^j-Low, BDT-Bin 0-4	$4.0^{+2.7}_{-2.0}$	$8.7^{+3.5}_{-2.8}$	1.53 ± 0.30	3.33 ± 0.32	2.83 ± 0.32	2.8 ± 0.4	1.9 ± 1.0
VBF-enriched p_T^j-Low, BDT-Bin 5-9	$2.4^{+2.0}_{-1.3}$	$5.7^{+2.8}_{-2.1}$	0.43 ± 0.11	9.6 ± 0.9	0.27 ± 0.04	0.153 ± 0.028	0.32 ± 0.17
VBF-enriched p_T^j-High	$0.6^{+1.3}_{-0.6}$	$2.8^{+2.1}_{-1.4}$	0.16 ± 0.05	1.18 ± 0.11	0.51 ± 0.06	0.71 ± 0.09	–
VH-Had enriched, BDT-Bin 0-4	$2.4^{+2.1}_{-1.4}$	$2.4^{+2.1}_{-1.4}$	1.00 ± 0.23	1.08 ± 0.13	1.52 ± 0.17	0.33 ± 0.07	0.9 ± 0.5
VH-Had enriched, BDT-Bin 5-9	$1.3^{+1.6}_{-0.9}$	0	0.37 ± 0.07	0.29 ± 0.06	5.0 ± 0.5	1.06 ± 0.19	0.29 ± 0.15
VH-Lep enriched	$0.3^{+1.0}$	0	–	–	2.94 ± 0.24	1.70 ± 0.19	–
ttH-enriched	$0.4^{+1.1}$	0	–	–	0.19 ± 0.04	13.5 ± 2.9	0.31 ± 0.17
Combined acceptance			23.5 ± 1.9	26.4 ± 1.4	22.3 ± 1.9	20.3 ± 2.0	24 ± 12

$H \to \gamma\gamma$ reco categories

Category	Selection
tH lep 0fwd	$N_{\rm lep} = 1$, $N_{\rm jets}^{\rm cen} \leq 3$, $N_{\rm b-tag} \geq 1$, $N_{\rm jets}^{\rm fwd} = 0$ ($p_{\rm T}^{\rm jet} > 25\,{\rm GeV}$)
tH lep 1fwd	$N_{\rm lep} = 1$, $N_{\rm jets}^{\rm cen} \leq 4$, $N_{\rm b-tag} \geq 1$, $N_{\rm jets}^{\rm fwd} \geq 1$ ($p_{\rm T}^{\rm jet} > 25\,{\rm GeV}$)
ttH lep	$N_{\rm lep} \geq 1$, $N_{\rm jets}^{\rm cen} \geq 2$, $N_{\rm b-tag} \geq 1$, $Z_{\ell\ell}$ veto ($p_{\rm T}^{\rm jet} > 25\,{\rm GeV}$)
ttH had BDT1	$N_{\rm lep} = 0$, $N_{\rm jets} \geq 3$, $N_{\rm b-tag} \geq 1$, ${\rm BDT_{ttH}} > 0.92$
ttH had BDT2	$N_{\rm lep} = 0$, $N_{\rm jets} \geq 3$, $N_{\rm b-tag} \geq 1$, $0.83 < {\rm BDT_{ttH}} < 0.92$
ttH had BDT3	$N_{\rm lep} = 0$, $N_{\rm jets} \geq 3$, $N_{\rm b-tag} \geq 1$, $0.79 < {\rm BDT_{ttH}} < 0.83$
ttH had BDT4	$N_{\rm lep} = 0$, $N_{\rm jets} \geq 3$, $N_{\rm b-tag} \geq 1$, $0.52 < {\rm BDT_{ttH}} < 0.79$
tH had 4j1b	$N_{\rm lep} = 0$, $N_{\rm jets}^{\rm cen} = 4$, $N_{\rm b-tag} = 1$ ($p_{\rm T}^{\rm jet} > 25\,{\rm GeV}$)
tH had 4j2b	$N_{\rm lep} = 0$, $N_{\rm jets}^{\rm cen} = 4$, $N_{\rm b-tag} \geq 2$ ($p_{\rm T}^{\rm jet} > 25\,{\rm GeV}$)
VH dilep	$N_{\rm lep} \geq 2$, $70\,{\rm GeV} \leq m_{\ell\ell} \leq 110\,{\rm GeV}$
VH lep HIGH	$N_{\rm lep} = 1$, $\lvert m_{e\gamma} - 89\,{\rm GeV}\rvert > 5\,{\rm GeV}$, $p_{\rm T}^{l+E_{\rm T}^{\rm miss}} > 150\,{\rm GeV}$
VH lep LOW	$N_{\rm lep} = 1$, $\lvert m_{e\gamma} - 89\,{\rm GeV}\rvert > 5\,{\rm GeV}$, $p_{\rm T}^{l+E_{\rm T}^{\rm miss}} < 150\,{\rm GeV}$, $E_{\rm T}^{\rm miss}$ significance > 1
VH MET HIGH	$150\,{\rm GeV} < E_{\rm T}^{\rm miss} < 250\,{\rm GeV}$, $E_{\rm T}^{\rm miss}$ significance > 9 or $E_{\rm T}^{\rm miss} > 250\,{\rm GeV}$
VH MET LOW	$80\,{\rm GeV} < E_{\rm T}^{\rm miss} < 150\,{\rm GeV}$, $E_{\rm T}^{\rm miss}$ significance > 8
jet BSM	$p_{\rm T,j1} > 200\,{\rm GeV}$
VH had tight	$60\,{\rm GeV} < m_{\rm jj} < 120\,{\rm GeV}$, ${\rm BDT_{VH}} > 0.78$
VH had loose	$60\ GeV < m_{\rm jj} < 120\,{\rm GeV}$, $0.35 < {\rm BDT_{VH}} < 0.78$
VBF tight, high p_T^{Hjj}	$\Delta\eta_{\rm jj} > 2$, $\lvert\eta_{\gamma\gamma} - 0.5(\eta_{\rm j1} + \eta_{\rm j2})\rvert < 5$, $p_T^{Hjj} > 25\,{\rm GeV}$, ${\rm BDT_{VBF}} > 0.47$
VBF loose, high p_T^{Hjj}	$\Delta\eta_{\rm jj} > 2$, $\lvert\eta_{\gamma\gamma} - 0.5(\eta_{\rm j1} + \eta_{\rm j2})\rvert < 5$, $p_T^{Hjj} > 25\,{\rm GeV}$, $-0.32 < {\rm BDT_{VBF}} < 0.47$
VBF tight, low p_T^{Hjj}	$\Delta\eta_{\rm jj} > 2$, $\lvert\eta_{\gamma\gamma} - 0.5(\eta_{\rm j1} + \eta_{\rm j2})\rvert < 5$, $p_T^{Hjj} < 25\,{\rm GeV}$, ${\rm BDT_{VBF}} > 0.87$
VBF loose, low p_T^{Hjj}	$\Delta\eta_{\rm jj} > 2$, $\lvert\eta_{\gamma\gamma} - 0.5(\eta_{\rm j1} + \eta_{\rm j2})\rvert < 5$, $p_T^{Hjj} < 25\,{\rm GeV}$, $0.26 < {\rm BDT_{VBF}} < 0.87$
ggH 2J BSM	≥ 2 jets, $p_{\rm T}^{\gamma\gamma} \geq 200\,{\rm GeV}$
ggH 2J HIGH	≥ 2 jets, $p_{\rm T}^{\gamma\gamma} \in [120, 200]$ GeV
ggH 2J MED	≥ 2 jets, $p_{\rm T}^{\gamma\gamma} \in [60, 120]$ GeV
ggH 2J LOW	≥ 2 jets, $p_{\rm T}^{\gamma\gamma} \in [0, 60]$ GeV
ggH 1J BSM	$= 1$ jet, $p_{\rm T}^{\gamma\gamma} \geq 200\,{\rm GeV}$
ggH 1J HIGH	$= 1$ jet, $p_{\rm T}^{\gamma\gamma} \in [120, 200]$ GeV
ggH 1J MED	$= 1$ jet, $p_{\rm T}^{\gamma\gamma} \in [60, 120]$ GeV
ggH 1J LOW	$= 1$ jet, $p_{\rm T}^{\gamma\gamma} \in [0, 60]$ GeV
ggH 0J FWD	$= 0$ jets, one photon with $\lvert\eta\rvert > 0.95$
ggH 0J CEN	$= 0$ jets, two photons with $\lvert\eta\rvert \leq 0.95$

Couplings and $\sigma \times$BR in the 4l channel

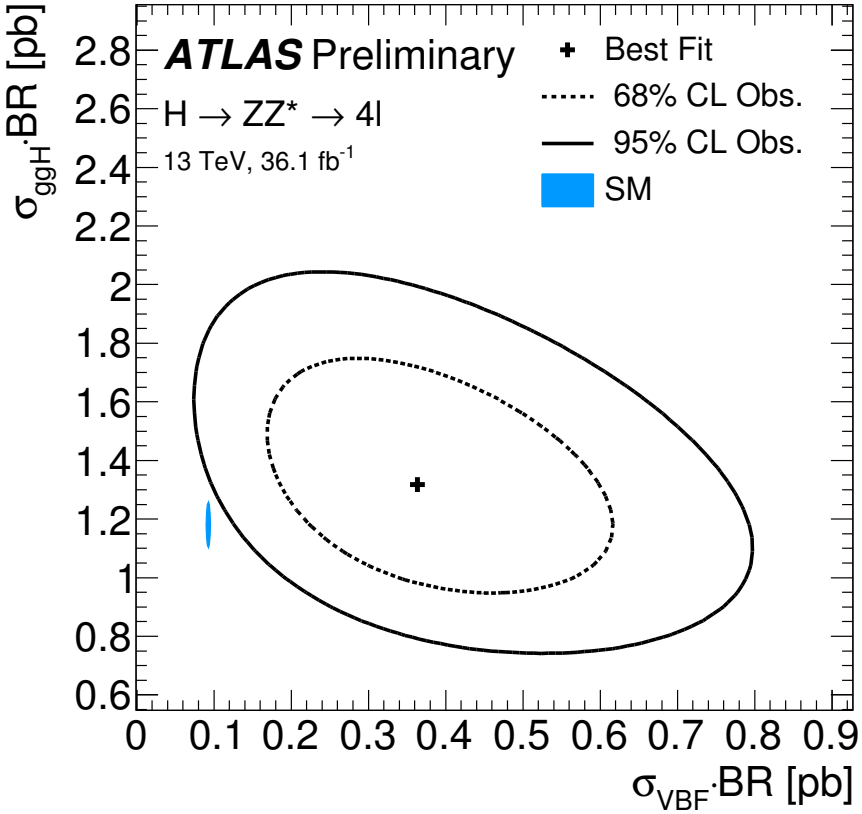

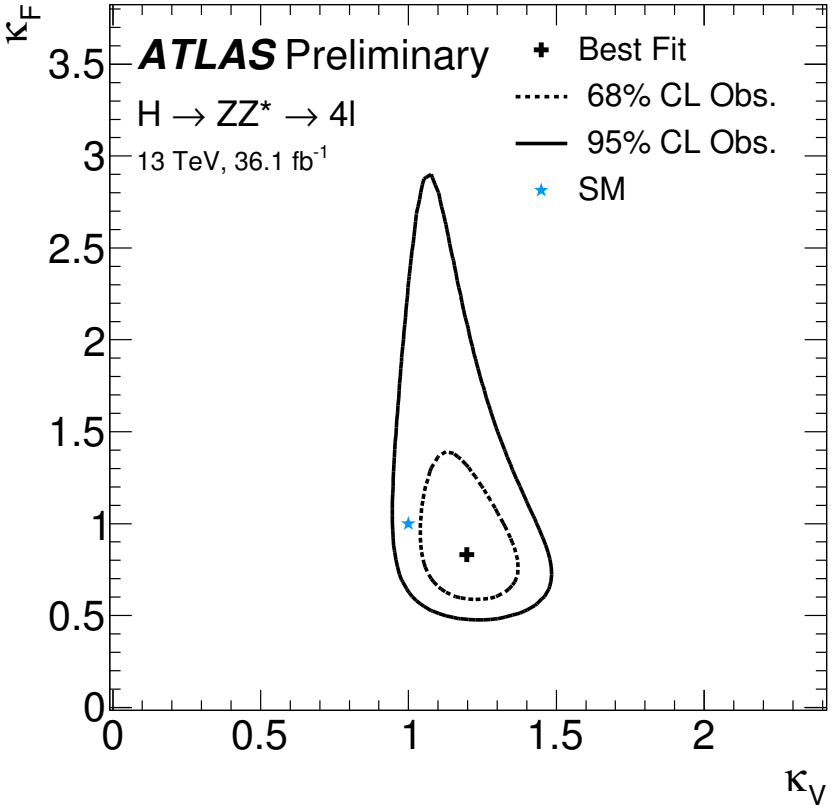

Cross Sections

Cross section [fb]	Data (± (stat) ± (sys))	LHCXSWG prediction	p-value [%]
$\sigma_{4\mu}$	$0.92\ ^{+0.25}_{-0.23}\ ^{+0.07}_{-0.05}$	0.880 ± 0.039	88
σ_{4e}	$0.67\ ^{+0.28}_{-0.23}\ ^{+0.08}_{-0.06}$	0.688 ± 0.031	96
$\sigma_{2\mu 2e}$	$0.84\ ^{+0.28}_{-0.24}\ ^{+0.09}_{-0.06}$	0.625 ± 0.028	39
$\sigma_{2e2\mu}$	$1.18\ ^{+0.30}_{-0.26}\ ^{+0.07}_{-0.05}$	0.717 ± 0.032	7
σ_{comb}	$3.62\ ^{+0.53}_{-0.50}\ ^{+0.25}_{-0.20}$	2.91 ± 0.13	18
σ_{tot} [pb]	$69\ ^{+10}_{-9}\ \pm 5$	55.6 ± 2.5	19

Fiducial region	Measured cross section	SM prediction	
Diphoton fiducial	54.7 ± 9.1 (stat.) ± 4.5 (syst.) fb	63.5 ± 2.4 fb	[N^{3}LO + XH]
VBF-enhanced	3.7 ± 0.8 (stat.) ± 0.5 (syst.) fb	2.24 ± 0.14 fb	[NNLOPS + XH]
$N_{\text{lepton}} \geq 1$	≤ 1.39 fb @ 95% CL	0.57 ± 0.03 fb	[NNLOPS + XH]
High $E_{\text{T}}^{\text{miss}}$	≤ 1.00 fb @ 95% CL	0.30 ± 0.02 fb	[NNLOPS + XH]
$t\bar{t}H$-enhanced	≤ 1.27 fb @ 95% CL	0.55 ± 0.05 fb	[NNLOPS + XH]

Decay channel	Total cross section ($pp \to H + X$)		
	$\sqrt{s}$ =7 TeV	$\sqrt{s}$ =8 TeV	$\sqrt{s}$ =13 TeV
$H \to \gamma\gamma$	35^{+13}_{-12} pb	$30.5^{+7.5}_{-7.4}$ pb	$47.9^{+9.1}_{-8.6}$ pb
$H \to ZZ^* \to 4\ell$	33^{+21}_{-16} pb	37^{+9}_{-8} pb	$68.0^{+11.4}_{-10.4}$ pb
Combination	34 ± 10 (stat.) $^{+4}_{-2}$ (syst.) pb	$33.3^{+5.5}_{-5.3}$ (stat.) $^{+1.7}_{-1.3}$ (syst.) pb	$57.0^{+6.0}_{-5.9}$ (stat.) $^{+4.0}_{-3.3}$ (syst.) pb
SM prediction [8]	19.2 ± 0.9 pb	24.5 ± 1.1 pb	$55.6^{+2.4}_{-3.4}$ pb

Couplings and $\sigma \times$BR in $\gamma\gamma$ channel

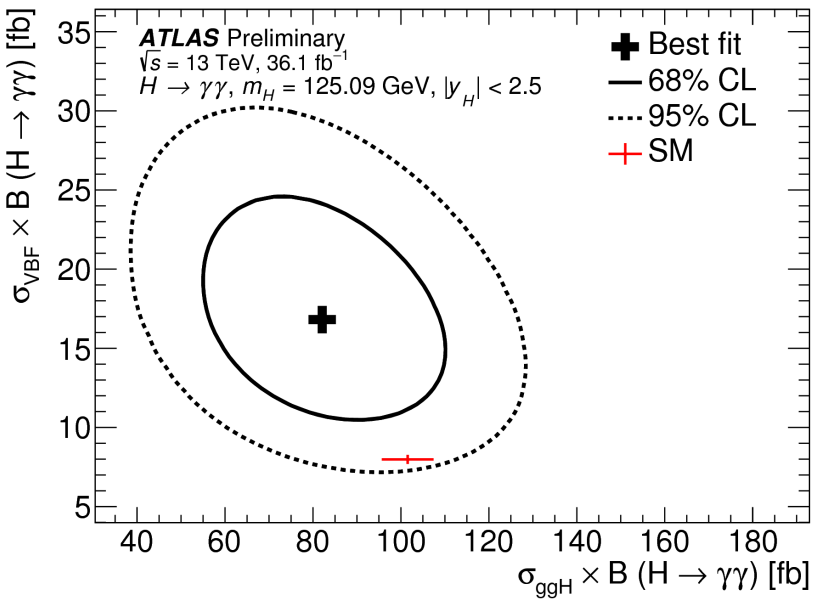

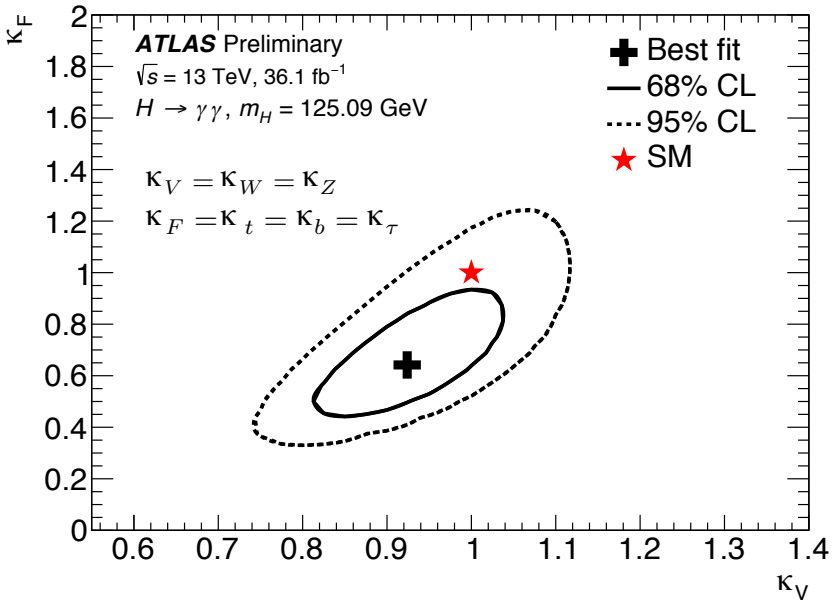

Effective Lagrangian of the Higgs characterization model

$$
\begin{aligned}
\mathcal{L}_0^V = \quad & \Big\{ \kappa_{\rm SM} \left[\tfrac{1}{2} g_{HZZ} Z_\mu Z^\mu + g_{HWW} W^+_\mu W^{-\mu} \right] \\
& - \tfrac{1}{4} \left[\kappa_{Hgg} g_{Hgg} G^a_{\mu\nu} G^{a,\mu\nu} + \tan\alpha \kappa_{Agg} g_{Agg} G^a_{\mu\nu} \tilde{G}^{a,\mu\nu} \right] \\
& - \tfrac{1}{4} \tfrac{1}{\Lambda} \left[\kappa_{HZZ} Z_{\mu\nu} Z^{\mu\nu} + \tan\alpha \kappa_{AZZ} Z_{\mu\nu} \tilde{Z}^{\mu\nu} \right] \\
& - \tfrac{1}{2} \tfrac{1}{\Lambda} \left[\kappa_{HWW} W^+_{\mu\nu} W^{-\mu\nu} + \tan\alpha \kappa_{AWW} W^+_{\mu\nu} \tilde{W}^{-\mu\nu} \right] \Big\} \mathcal{X}_0 . \qquad (1)
\end{aligned}
$$

Limits on EFT couplings

BSM coupling κ_{BSM}	Fit configuration	Expected limit	Observed limit	Best-fit $\hat{\kappa}_{\mathrm{BSM}}$	Best-fit $\hat{\kappa}_{\mathrm{SM}}$	Deviation from SM
κ_{Agg}	($\kappa_{Hgg} = 1$, $\kappa_{\mathrm{SM}} = 1$)	[-0.47, 0.47]	[-0.68, 0.68]	± 0.43	-	1.8σ
κ_{HVV}	($\kappa_{Hgg} = 1$, $\kappa_{\mathrm{SM}} = 1$)	[-2.9, 3.2]	[0.8, 4.5]	2.9	-	2.3σ
κ_{HVV}	($\kappa_{Hgg} = 1$, κ_{SM} free)	[-3.1, 4.0]	[-0.6, 4.2]	2.2	1.2	1.7σ
κ_{AVV}	($\kappa_{Hgg} = 1$, $\kappa_{\mathrm{SM}} = 1$)	[-3.5, 3.5]	[-5.2, 5.2]	± 2.9	-	1.4σ
κ_{AVV}	($\kappa_{Hgg} = 1$, κ_{SM} free)	[-4.0, 4.0]	[-4.4, 4.4]	± 1.5	1.2	0.5σ

Fit configuration	Best-fit $\hat{\kappa}_{HVV}$	Best-fit $\hat{\kappa}_{AVV}$	Best-fit $\hat{\kappa}_{\mathrm{SM}}$	Deviation from SM
$\kappa_{Hgg} = 1$, $\kappa_{\mathrm{SM}} = 1$	2.9	± 0.5	-	1.9σ
$\kappa_{Hgg} = 1$, κ_{SM} free	2.1	± 0.3	1.7	1.2σ